# Adaptive Formation Tracking Control for First-Order Agents with a Time-Varying Flow Parameter

Yang-Yang Chen, *Member, IEEE*, Kaiwen Chen, and Alessandro Astolfi, *Fellow, IEEE*

***Abstract*— A novel adaptive method to achieve both path following and formation moving along desired orbits in the presence of a spatio-temporal flowfield is presented. The flowfield is a spatio-temporal general flow with unknown time-varying parameters. The so-called *congelation of variables* method is used to estimate the time-varying flow parameters, which do not have any restrictions on the rate of their variation. The asymptotic properties of the resulting adaptive system are studied in detail. Simulation results demonstrate the effectiveness of the proposed method.**

***Index Terms*— Formation tracking control, time-varying flow parameters, adaptive estimate.**

## I. Introduction

Formation tracking control, also called as coordinated path following control, has received significant attention in oceanic and planetary explorations [1], [2]. Differently from the consensus problem [3], [4], the objective of the formation tracking control problem consists of the simultaneous path following and formation control around a given orbit. This yields, for example, good performance in seeking measurements of biological variables across a range of spatial and temporal scales [5]. In early works on formation tracking control, see e.g. [6]–[9], the effect of the external flowfield has been ignored. However, as pointed out in [10], the flowfield may force the vehicles to deviate from the desired orbit and may affect the formation to such an extent that it can cause damage to the equipment [11]. It is therefore essential to design formation tracking methods in the presence of a flowfield.

In the area of flow-based formation tracking control there are two main trends. The first is based on state/parameter estimation methods. In particular, a state observer to achieve even distribution on a simple and closed curve with an unknown time-invariant flowfield is given in [12]. A similar idea is used in [13], in which the flowfield is uniformly rotating with an unknown rotating speed. In [14] a consensus-based filter to estimate the uncertain constant parameter of the parameterized flowfield, under the assumption that the convergence speed of the filter is faster than that of the tracking error, is designed. Formation tracking in a general flowfield has been studied with a new adaptive method in [15], on the basis of the notion of neighbor states, whereas a disturbance observer has been proposed in [16] to estimate disturbances, the time derivative of which converges to zero. An alternative filter to deal with unknown nonlinear terms satisfying a Lipschiz-like condition has been designed in [17]. Finally, adaptive methods have been applied to cooperative output regulation in [18] and to the unknown target enclosing task in [19]. However, none of the aforementioned methods is applicable to the case in which the parameter is time-varying and the rate of its variation has no restriction.

The second trend is based on the use of adaptive neural network (ANN). In the 1990's, ANNs have been introduced for flight control problems [20]. In [21], the formation flight control problem with uncertainties has been translated into a simple master-slave tracking control problem and it has then be solved with an ANN. Such a method is developed for the general leader-following structure in [22] and in [23] for ocean currents. ANNs have also proven to be useful to deal with time-delays in multi-agent systems [24], for robust time-varying formation mission [25] and in the case of topology-switching multi-agent systems [26]. It should be noted that the use of ANNs is beneficial in the presence of nonlinearity and in dealing with spacial flowfields. However it cannot be used to address the formation tracking problem in spatio-temporal flowfields. Finally by using ANNs only uniform boundedness of the tracking error can be obtained. In practice, the dynamics of the flowfield is often spatio-temporal and contains unknown time-varying parameters [27], the effect of which cannot be alleviated by the indicated estimation methods and/or by the use of ANNs.

Recently a novel method called *congelation of variables* [28]–[31] has been developed for the adaptive stabilization of a class of single-input-single-output nonlinear system with time-varying parameters. On the basis of this adaptive method we propose a novel robust formation tracking control for bidirectional connected first-order agents. The flowfield under consideration is a general spatio-temporal flow with unknown time-varying parameters: this can model for example the time-varying spatially flowfield in [13], the parameterizable flowfield in [14], [15] and the Eulerian flowfield in [32]. The formation tracking task with/without reference orbital speed is addressed and solved by means of a *congelation of variables* method, with asymptotic guarantees, despite the effect of a state and time dependant spatio-temporal flow. In addition, the adaptive update law for the unknown time-varying parameters in the case of formation tracking without reference orbital speed is designed by using the consensus errors, i.e. the differences between neighboring states, yielding an adaptive update law different form that in [31]. Note finally that the class of systems studied in this paper is different from that in [31].

The paper is organized as follows. Section II summarizes some preliminaries and formulates the adaptive tracking control problem in the presence of an unknown spatio-temporal flowfield. In Section III we firstly give a solution to the problem in which a reference orbital speed is given and then we solve the problem without the use of any global reference signals. Simulation results are presented in Section IV. Conclusions are given in Section V.

This work has been partially supported by the National Natural Science Foundation of China under Grant 61673106, Natural Science Foundation of Jiangsu Province under Grant BK20171362, the European Union's Horizon 2020 Research and Innovation Programme under grant agreement No 739551 (KIOS CoE), and by Italian Ministry for Research in the framework of the 2017 Program for Research Projects of National Interest (PRIN), Grant no. 2017YKXYXJ.

Y.-Y. Chen is with School of Automation and Key Laboratory of Measurement and Control of Complex Systems of Engineering, Ministry of Education, Southeast University, Nanjing 210096, China, (e-mail: yychen@seu.edu.cn).

K. Chen is with the Department of Electrical and Electronic Engineering, Imperial College London, London, SW7 2AZ, U.K. (e-mail: kaiwen.chen16@imperial.ac.uk).

A. Astolfi is with the Department of Electrical and Electronic Engineering, Imperial College London, London, SW7 2AZ, U.K., and also with the Department of Civil Engineering and Computer Science Engineering, University of Rome Tor Vergata, 00133 Rome, Italy (e-mail: a.astolfi@imperial.ac.uk).

## II. Preliminaries and Problem Statement

### A. Preliminaries

The notation used in the paper is standard. $\mathbb{R}$ denotes the set of real numbers. $\mathbb{T}$ denotes the one-torus, that is, $\phi \in \mathbb{T}$ implies that we identify $\phi + 2\pi$ with $\phi$. $\|\cdot\|$ denotes the Euclidean norm and $|M|$ denotes the determinant of the square matrix $M$.

Let $\mathcal{G} = \{\mathcal{V}, \mathcal{E}\}$ be a bidirectional graph defining a network topology among vehicles. The set $\mathcal{V} = \{\mathcal{V}_1, \cdots, \mathcal{V}_n\}$ denotes a set of $n$ vehicles and $\mathcal{E} \subseteq \mathcal{V} \times \mathcal{V}$ is a set of data links. A path from node $\mathcal{V}_j$ to $\mathcal{V}_i$ is a sequence of edges $(\mathcal{V}_i, \mathcal{V}_{i_1}), \ldots, (\mathcal{V}_{i_m}, \mathcal{V}_j)$ in the network topology with distinct nodes $\mathcal{V}_{i_k}, k = 1, \ldots, m$. A bidirectional topology is connected if there exists a path from any node to any other nodes in the graph. Let, for $i, j = 1, \ldots, n$, $a_{ii} = 0$, $a_{ij} = a_{ji} = 1$ if $(\mathcal{V}_j, \mathcal{V}_i) \in \mathcal{E}$, and $a_{ij} = 0$ otherwise. In addition define the Laplacian matrix $L \triangleq [l_{ij}]_{i,j=1}^n$ with $l_{ii} = \sum_{j=1}^n a_{ij}$ and $l_{ij} = -a_{ij}$, for any $i \neq j$, $i, j = 1, \ldots, n$.

In this paper the desired orbit associated to each vehicle is a simple, closed and regular curve with nonzero curvature. In a fixed inertial reference frame it can be parameterized by a smooth map $\mathcal{C}_{i0} : [0, 2\pi) \to \mathbb{R}^2$, $\phi_i \mapsto \mathcal{C}_{i0}(\phi_i)$, where $\phi_i \in \mathbb{T}$ is the phase angle denoting the direction of the vector from the origin of the orbit to the point on the orbit with respect to the positive axis of the fixed inertial reference frame. To define each desired orbit as a level line of the smooth map $\mathcal{C}_{i0}$ should satisfy the following additional conditions, in which $\varepsilon$ is a positive constant.

(C1) $\|\mathcal{C}_{i0}(\phi_i)\| > \varepsilon \geq 0$, which means that the distance from each point on the orbit to the origin of the fixed inertial reference is bounded away from zero. This assumption is without loss of generality, since one can always shift the origin of the reference frame.

(C2) $0 < \varepsilon \leq \|\mathbf{d}\mathcal{C}_{i0}(\phi_i)/\mathbf{d}\phi_i\| < \infty$, which implies that the tangent vector at each point of the orbit is well-defined and nonzero.

(C3) $|\mathcal{C}_{i0}(\phi_i), \mathbf{d}\mathcal{C}_{i0}(\phi_i)/\mathbf{d}\phi_i| \neq 0$ for all $\phi_i$, which implies that the well-defined vector from the origin to each point $p_{i,k}$ on the orbit and the tangent vector to the orbit at $p_{i,k}$ are linearly independent.

If the above assumptions hold a set of level curves of a smooth function can be constructed by concentric compression, that is by defining the maps

$$\mathcal{C}_{ic}(\phi_i, c) = (1 - c)\,\mathcal{C}_{i0}(\phi_i), \tag{1}$$

where $c \in \mathbb{R}$ is the compression margin.

*Lemma 1 [8]:* For any simple, closed and regular orbit satisfying conditions (C1) to (C3) and identified by the map $\mathcal{C}_{i0}$, there exists a constant $\varepsilon_i > 0$ such that $\mathcal{C}_{i(\cdot)}(\cdot, \cdot)$ is a diffeomorphism on $[0, 2\pi) \times (-\varepsilon_i, \varepsilon_i)$. Moreover there exists an open set $\Omega_i \subset \mathbb{R}^2$, which is a tubular neighborhood of the orbit, and a smooth function $\lambda_i : \Omega_i \to (-\varepsilon_i, \varepsilon_i)$, which is called the *orbit function* (and its value is called the orbit value), such that the following conditions hold:

1. $\|\nabla\lambda_i\| = \left\|\frac{\partial\lambda_i}{\partial p_i}\right\| \neq 0$, for all $p_i \in \Omega_i$;
2. $\lambda_i(p_i) = c$, for all point $p_i$ on the orbit identified by $\mathcal{C}_{ic}$ with $c \in (-\varepsilon_i, \varepsilon_i)$.

*Remark 1:* $\mathcal{C}_{ic}$ is a level line of the orbit function $\lambda_i(p_i)$ and the orbit value associated to the orbit $\mathcal{C}_{i0}$ is zero, as illustrated in Figure 1.

*Remark 2:* The (skewed) superellipse, a class of closed curves that includes circles, ellipses, and rounded parallelograms, is described via the equation

$$\mathcal{C}_{i0}(\phi_i) = \left[a(\cos\phi_i)^{\frac{1}{\nu}} + \mu b(\sin\phi_i)^{\frac{1}{\nu}}, b(\sin\phi_i)^{\frac{1}{\nu}}\right]^T, \tag{2}$$

where $\mu \in \mathbb{R}$ is the so-called skewness parameter. The semi-major axis length $a$ and the semi-minor axis length $b$ satisfy $a \geqslant b > 0$.

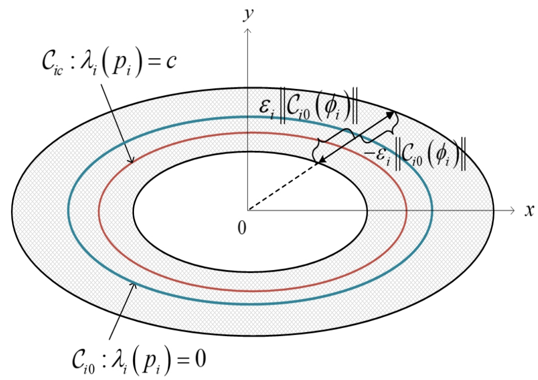


Fig. 1. Level orbits of $\boldsymbol{\lambda_i(p_i)}$ on $\boldsymbol{\Omega_i}$. The meshed area denotes the tubular neighborhood $\boldsymbol{\Omega_i}$.

The parameter $\nu = 1, 3, 5, \ldots$ determines the corner sharpness. For $\mu = 0$ and $a > b$ (resp. $a = b$), setting $\nu = 1$ yields an ellipse (resp. a circle) and setting $\nu \geq 3$ yields a *rounded rectangle* (resp. a *rounded square*). Setting $\mu \neq 0$ and $\nu > 1$ yields a *rounded parallelogram*. Note now that equation (1) yields

$$\begin{aligned}\mathcal{C}_{i\lambda}(\phi_i, c) &= [p_{x_i}(\phi_i, c), p_{y_i}(\phi_i, c)]^T \\ &= \begin{bmatrix} (1-c)\left(a(\cos\phi_i)^{\frac{1}{\nu}} + \mu b(\sin\phi_i)^{\frac{1}{\nu}}\right) \\ (1-c)\, b(\sin\phi_i)^{\frac{1}{\nu}} \end{bmatrix}.\end{aligned} \tag{3}$$

Thus, using equation (3) we obtain

$$\left(\frac{p_{x_i} - \mu p_{y_i}}{a}\right)^{2\nu} + \left(\frac{p_{y_i}}{b}\right)^{2\nu} = (1-c)^{2\nu}, \tag{4}$$

which, solved for $c$, gives the expression of the orbit function, that is

$$\lambda_i(p_i) = c = 1 - \left(\left(\frac{p_{x_i} - \mu p_{y_i}}{a}\right)^{2\nu} + \left(\frac{p_{y_i}}{b}\right)^{2\nu}\right)^{\frac{1}{2\nu}}. \tag{5}$$

As a result, the tubular neighborhood can be represented as

$$\Omega_i = \left\{p_i \in \mathbb{R}^2 \mid |\lambda_i(p_i)| < \varepsilon_i\right\}$$

with $0 < \varepsilon_i < 1$. Note finally that

$$\begin{aligned}\left\|\frac{\partial\lambda_i}{\partial p_i}\right\| = (1-\lambda_i)^{1-2\nu}\Bigg[&\frac{1}{a^2}\left(\frac{p_{x_i} - \mu p_{y_i}}{a}\right)^{4\nu-2} \\ &+ \frac{\mu^2}{a^2}\left(\frac{p_{x_i} - \mu p_{y_i}}{a}\right)^{4\nu-2} + \frac{1}{b^2}\left(\frac{p_{y_i}}{b}\right)^{4\nu-2} \\ &-2\frac{\mu}{ab}\left(\frac{p_{x_i} - \mu p_{y_i}}{a}\right)^{2\nu-1}\left(\frac{p_{y_i}}{b}\right)^{2\nu-1}\Bigg]^{\frac{1}{2}}.\end{aligned} \tag{6}$$

Hence $\|\nabla\lambda_i\|$ is bounded on the set $\Omega_i$. For illustration Figure 2 displays level superellipses with $a = 3$, $b = 3$, $\mu = 0$, $\nu = 3$ and $c = -0.5$, $c = 0$, and $c = 0.5$.

To ensure that each vehicle with initial position in $\Omega_i$ remains in $\Omega_i$, a barrier function $\Psi_i$ is introduced.

*Definition 1:* A $C^2$ function $\Psi_i : (-\varepsilon_i, \varepsilon_i) \to \mathbb{R}$ is a barrier function with a wide of $2\varepsilon_i$ if

(C4) $\lim_{\lambda_i \to -\varepsilon_i^+} \Psi_i(\lambda_i) = +\infty$ and $\lim_{\lambda_i \to -\varepsilon_i^+} \nabla\Psi_i(\lambda_i) = -\infty$.

(C5) $\lim_{\lambda_i \to \varepsilon_i^-} \Psi_i(\lambda_i) = +\infty$ and $\lim_{\lambda_i \to \varepsilon_i^-} \nabla\Psi_i(\lambda_i) = +\infty$.

(C6) $\nabla\Psi_i(0) = 0$.

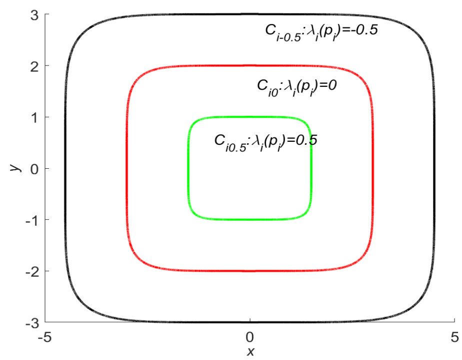


Fig. 2. Plots of level superellipses.

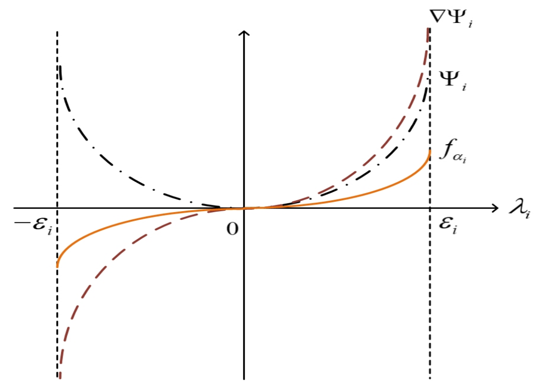


Fig. 3. Sketches of $\Psi$, $\nabla\Psi_i$ and $f_{\alpha_i}$.

## B. Problem statement

Consider a formation composed of $n$ vehicles moving in a fixed inertial reference frame each satisfying the dynamic equation

$$\dot{p}_i = u_i + f_i\left(p_i, t, \theta_i\left(t\right)\right), \tag{7}$$

with position variable $p_i(t) \in \mathbb{R}^2$, and control input $u_i = [u_{x_i}, u_{y_i}]^T \in \mathbb{R}^2$. The mapping $f_i\left(p_i, \theta_i\left(t\right)\right)$ denotes the spatio-temporal flowfield which is such that

$$f_i\left(p_i, t, \theta_i\left(t\right)\right) = f_{\alpha_i}\left(\lambda_i\right) f_{\beta_i}\left(p_i, t\right) \theta_i\left(t\right), \tag{8}$$

where $f_{\alpha_i} : \mathbb{R} \to \mathbb{R}$ denotes the known, space-based flow amplitude; $f_{\beta_i} : \mathbb{R}^2 \times \mathbb{R} \to \mathbb{R}^{2\times m}$ is the $2 \times m$ matrix of known basis bounded functions of the flowfield; and $\theta_i\left(t\right) \in \mathbb{R}^m$ is the set of unknown time-varying parameters.

*Assumption 1:* The functions $f_{\alpha_i}$ are bounded and are such that $\nabla\Psi_i f_{\alpha_i} \geq f_{\alpha_i}^2$, for all $\lambda_i$, and $f_{\alpha_i}(0) = 0$.

*Assumption 2:* There exists a constant $c_1 > 0$ such that $\left\|f_{\beta_i}\right\| \leq c_1$, for all $p_i$ and $t \geq 0$.

*Assumption 3:* The vectors of unknown time-varying parameters $\theta_i\left(t\right)$ satisfy, for all $t \geq 0$, the box constraint

$$\underline{\theta}_i \leq \theta_i\left(t\right) \leq \bar{\theta}_i, \tag{9}$$

for some constants $\underline{\theta}_i \in \mathbb{R}^m$ and $\bar{\theta}_i \in \mathbb{R}^m$ where the sign $\leq$ is defined element-wise. Moreover the *radius* of the box $\delta_{i*} = \frac{1}{2}\left|\bar{\theta}_i - \underline{\theta}_i\right|$ is known.

*Remark 3:* Figure 3 provides a graphical illustration of the relation among $\Psi_i$, $\nabla\Psi_i$ and $f_{\alpha_i}$. Some examples of barrier functions $\Psi_i$ can be found in [8]. Note that it is always possible to construct a barrier function such that Assumption 1 holds.

*Remark 4:* Assumption 1 is without loss of generality. Choosing the functions $f_\alpha$ such that the signs of $f_\alpha$ and $\nabla\Psi_i$ are consistent and noting that

$$\begin{aligned} f_i\left(p_i, t, \theta_i\left(t\right)\right) &= f_{\alpha_i}\left(\lambda_i\right) f_{\beta_i}\left(p_i, t\right) \theta_i\left(t\right) \\ &= \left(\alpha_i \bar{f}_{\alpha_i}\left(\lambda_i\right)\right)\left(\alpha_i^{-1} \bar{f}_{\beta_i}\left(p_i, t\right)\right) \theta_i\left(t\right), \end{aligned}$$

the condition $\nabla\Psi_i f_{\alpha_i} \geq f_{\alpha_i}^2$, for all $\lambda_i \in (-\varepsilon_i, \varepsilon_i)$ can be enforced by adjusting the parameter $0 < \alpha_i < 1$. Moreover since the flowfields $f_i$ are bounded, it is natural to assume that the functions $f_{\alpha_i}$ are bounded. The condition $f_{\alpha_i}\left(0\right) = 0$ implies that the effect of the flowfield disappears on the desired orbit associated to each vehicle.

*Remark 5:* Assumption 2 is natural due to boundedness of the flowfields. Assumption 3 is a boundedness condition for the set of unknown time-varying parameters, which is natural and common in the literature, see e.g. [13]–[15] and [32].

The formation tracking objectives can be decomposed into a path following task and a formation motion task, which are formally described as follows.

The path following error can be described, by Lemma 1, as $\lambda_i(p_i(t))$, hence path following is achieved if

$$\lim_{t\to\infty} \lambda_i(p_i(t)) = 0, \tag{10}$$

and

$$\lambda_i(t) \in \Omega_i, \tag{11}$$

for all $t \geq 0$, where $\Omega_i = \left\{p_i \in \mathbb{R}^2 \mid \left|\lambda_i\left(p_i(t)\right)\right| < \varepsilon_i\right\}$.

To define the formation motion task the following definition of arc-lengthes $s_i$ should be given at first, i.e.,

$$s_i\left(\lambda_i, \phi_i\right) \triangleq \int_{\phi_i^*}^{\phi_i} \frac{\partial s_i\left(\lambda_i, \tau\right)}{\partial\tau} d\tau, \tag{12}$$

where $\phi_i^*$ is the parameter associated with the starting point of the arc.

Then, consistently with [8], the generalized arc-lengths $\xi_i(s_i)$ are $C^1$ functions of $s_i$ and $\left|\partial\xi_i/\partial s_i\right| \geq \varepsilon > 0$, which are selected to satisfy that formation is achieved if

$$\lim_{t\to\infty} \left(\xi_i(t) - \xi_j(t)\right) = 0. \tag{13}$$

Finally, the following assumption holds.

*Assumption 4:* The bidirectional topology associated with the $n$ vehicle system is fixed and connected.

In this paper the formation tracking problems with/without reference orbital speed are studied. These can be be formulated as follows.

*Problem 1. Adaptive formation tracking problem with reference orbital speed.* Let $i \in [1, n]$. Consider the system (8) and the initial position $p_i(0) \in \Omega_i$. Suppose Assumptions 1 to 4 hold. Design a formation tracking control law $u_i$, with an adaptive update law for the unknown time-varying flow parameter $\theta_i\left(t\right)$, such that the closed-loop system satisfies the control objectives (10), (11) and

$$\lim_{t\to\infty} \left(\xi_i\left(t\right) - \xi_*(t)\right) = 0, \tag{14}$$

where $\xi_*(t) = \int_o^t \eta_*(\tau)d\tau$, and $\eta_*(t) > 0$ is a bounded reference orbital speed.

*Problem 2. Adaptive formation tracking problem without reference orbital speed.* Let $i \in [1, n]$. Consider the system (8) and the initial position $p_i(0) \in \Omega_i$. Suppose Assumptions 1 to 4 hold. Design a formation tracking control law $u_i$, with an adaptive update law for the unknown time-varying flow parameter $\theta_i\left(t\right)$, such that the closed-loop system satisfies the control objectives (10), (11) and (13).

# III. Main Results

## A. Open-loop System

By Lemma 1 one obtains the path following dynamics by differentiating $\lambda_i$, i.e.[1],

$$\dot{\lambda}_i = \|\nabla\lambda_i\| v_{N_i} + f_{\alpha_i} \|\nabla\lambda_i\| f_{\beta_{Ni}}\theta_i, \tag{15}$$

where

$$v_{N_i} = N_i^T v_i \tag{16}$$

denotes the control input projected to the normal vector $N_i$ to the level orbit of the current position of the vehicle, $N_i = \frac{\nabla\lambda_i}{\|\nabla\lambda_i\|}$ and $f_{\beta_{Ni}} = N_i^T f_{\beta_i}$.

From (12) we have that

$$\dot{s}_i = v_{T_i} + f_{\alpha_i} f_{\beta_{Ti}}\theta_i + \frac{\partial s_i}{\partial\lambda_i}\|\nabla\lambda_i\| v_{N_i} + \frac{\partial s_i}{\partial\lambda_i} f_{\alpha_i}\|\nabla\lambda_i\| f_{\beta_{Ni}}\theta_i, \tag{17}$$

where

$$v_{T_i} = T_i^T v_i \tag{18}$$

denotes the control input projected to the tangent vector $T_i$ to the level orbit of the current position of the vehicle, $T_i = [R_1, R_2]^T N_i$ with $R_1 = [0,1]^T$ and $R_2 = [-1,0]^T$, and $f_{\beta_{Ti}} = T_i^T f_{\beta_i}$.

As a result, the dynamics of $\xi_i$ is given by the equation

$$\dot{\xi}_i = \frac{\partial\xi_i}{\partial s_i}\left(v_{T_i} + \frac{\partial s_i}{\partial\lambda_i}\|\nabla\lambda_i\| v_{N_i} + f_{\alpha_i}\left(f_{\beta_{Ti}} + \frac{\partial s_i}{\partial\lambda_i}\|\nabla\lambda_i\| f_{\beta_{Ni}}\right)\theta_i\right). \tag{19}$$

Therefore, the dynamics associated to the formation tracking system for the $i$th vehicle are described by equations (15) and (19).

## B. Solution to Problem 1

Let us consider the candidate Lyapunov function

$$V_I = \sum_{i=1}^n \Psi(\lambda_i) + \frac{1}{2}\sum_{i=1}^n \tilde{\xi}_i^2 + \frac{1}{\gamma}\sum_{i=1}^n \left(l_i - \hat{\theta}_i\right)^T\left(l_i - \hat{\theta}_i\right), \tag{20}$$

where $\tilde{\xi}_i = \xi_i - \xi_*$. The vector $l_i$ can be selected such that $l_i = \frac{1}{2}\left(\bar{\theta}_i + \underline{\theta}_i\right)$ as in [28], $\gamma > 0$ is the adaptation gain and $\hat{\theta}_i$ is the estimate of $\theta_i$.

In (20) the first term contributes to achieving the path following objective, i.e., equations (10) and (11). It vanishes when $\lambda_i = 0$. The second term contributes to achieving the desired formation, i.e., equation (14). The last term contributes to achieving flow estimation. Differentiating both sides of (20) along the trajectories of the system yields

$$\begin{aligned}\dot{V}_I &= \sum_{i=1}^n \nabla\Psi_i\left[\|\nabla\lambda_i\| v_{N_i} + f_{\alpha_i}\|\nabla\lambda_i\| f_{\beta_{Ni}}\theta_i\right] \\ &\quad + \sum_{i=1}^n \tilde{\xi}_i\left[\frac{\partial\xi_i}{\partial s_i}\left(v_{T_i} + \frac{\partial s_i}{\partial\lambda_i}\|\nabla\lambda_i\| v_{N_i} + f_{\alpha_i}\left(f_{\beta_{Ti}} + \frac{\partial s_i}{\partial\lambda_i}\|\nabla\lambda_i\| f_{\beta_{Ni}}\right)\theta_i\right) - \eta_*\right] - \frac{1}{\gamma}\sum_{i=1}^n\left(l_i - \hat{\theta}_i\right)^T\dot{\hat{\theta}}_i \\ &= \sum_{i=1}^n \nabla\Psi_i\left[\|\nabla\lambda_i\| v_{N_i} + f_{\alpha_i}\|\nabla\lambda_i\| f_{\beta_{Ni}}\left(\theta_i - l_i + l_i - \hat{\theta}_i + \hat{\theta}_i\right)\right] + \sum_{i=1}^n \tilde{\xi}_i\left[\frac{\partial\xi_i}{\partial s_i}\left(v_{T_i} + \frac{\partial s_i}{\partial\lambda_i}\|\nabla\lambda_i\| v_{N_i}\right.\right. \\ &\quad \left.\left. + f_{\alpha_i}\left(f_{\beta_{Ti}} + \frac{\partial s_i}{\partial\lambda_i}\|\nabla\lambda_i\| f_{\beta_{Ni}}\right)\left(\theta_i - l_i + l_i - \hat{\theta}_i + \hat{\theta}_i\right)\right) - \eta_*\right] - \frac{1}{\gamma}\sum_{i=1}^n\left(l_i - \hat{\theta}_i\right)^T\dot{\hat{\theta}}_i. \end{aligned} \tag{21}$$

Rewriting (21) as

$$\begin{aligned}\dot{V}_I &= \sum_{i=1}^n \nabla\Psi_i\left[\|\nabla\lambda_i\| v_{N_i} + f_{\alpha_i}\|\nabla\lambda_i\| f_{\beta_{Ni}}\left(\theta_i - l_i + \hat{\theta}_i\right)\right] \\ &\quad + \sum_{i=1}^n \tilde{\xi}_i\left[\frac{\partial\xi_i}{\partial s_i}\left(v_{T_i} + \frac{\partial s_i}{\partial\lambda_i}\|\nabla\lambda_i\| v_{N_i} + f_{\alpha_i}\right.\right. \\ &\quad \left.\left.\times\left(f_{\beta_{Ti}} + \frac{\partial s_i}{\partial\lambda_i}\|\nabla\lambda_i\| f_{\beta_{Ni}}\right)\left(\theta_i - l_i + \hat{\theta}_i\right)\right) - \eta_*\right] \\ &\quad + \sum_{i=1}^n\left(l_i - \hat{\theta}_i\right)^T\left[-\frac{1}{\gamma}\dot{\hat{\theta}}_i + \nabla\Psi_i f_{\alpha_i}\|\nabla\lambda_i\| f_{\beta_{Ni}}^T + \tilde{\xi}_i\frac{\partial\xi_i}{\partial s_i} f_{\alpha_i}\left(f_{\beta_{Ti}}^T + \frac{\partial s_i}{\partial\lambda_i}\|\nabla\lambda_i\| f_{\beta_{Ni}}^T\right)\right], \end{aligned} \tag{22}$$

suggests the selection

$$v_{N_i} = -\frac{1}{\|\nabla\lambda_i\|}\left(f_{\alpha_i}\|\nabla\lambda_i\| f_{\beta_{Ni}}\hat{\theta}_i + k_1 f_{\alpha_i}\right), \tag{23}$$

$$v_{T_i} = -f_{\alpha_i}\left(f_{\beta_{Ti}} + \frac{\partial s_i}{\partial\lambda_i} f_{\alpha_i}\|\nabla\lambda_i\| f_{\beta_{Ni}}\right)\hat{\theta}_i - \frac{\partial s_i}{\partial\lambda_i}\|\nabla\lambda_i\| v_{N_i} + \left(\frac{\partial\xi_i}{\partial s_i}\right)^{-1}\left(\eta_* - k_2\tilde{\xi}_i - k_3\sum_{j=1}^n a_{ij}\left(\xi_i - \xi_j\right)\right), \tag{24}$$

$$\dot{\hat{\theta}}_i = \gamma\left(\nabla\Psi_i f_{\alpha_i}\|\nabla\lambda_i\| f_{\beta_{Ni}}^T + \tilde{\xi}_i\frac{\partial\xi_i}{\partial s_i} f_{\alpha_i}\left(f_{\beta_{Ti}}^T + \frac{\partial s_i}{\partial\lambda_i}\|\nabla\lambda_i\| f_{\beta_{Ni}}^T\right)\right), \tag{25}$$

in which the control parameters $k_1$ and $k_2$ have to be selected and $k_3 > 0$. Substituting (23), (24) and (25) into (22) yields

$$\begin{aligned}\dot{V}_I &= \sum_{i=1}^n \nabla\Psi_i\left[-k_1\nabla\psi_i f_{\alpha_i} + f_{\alpha_i}\|\nabla\lambda_i\| f_{\beta_{Ni}}(\theta_i - l_i)\right] \\ &\quad + \sum_{i=1}^n \tilde{\xi}_i\left[\frac{\partial\xi_i}{\partial s_i} f_{\alpha_i}\left(f_{\beta_{Ti}} + \frac{\partial s_i}{\partial\lambda_i}\|\nabla\lambda_i\| f_{\beta_{Ni}}\right)(\theta_i - l_i) - k_2\tilde{\xi}_i - k_3\sum_{j=1}^n a_{ij}\left(\xi_i - \xi_j\right)\right]. \end{aligned} \tag{26}$$

Note that the closed-loop equations associated to the formation

[1] In what follows, to simplify notation, we use $\theta_i$ to denote $\theta_i(t)$.

tracking control system for the $i$th vehicle are

$$\begin{aligned}\dot{\lambda}_i &= -k_1 f_{\alpha_i} + f_{\alpha_i}\left\|\nabla\lambda_i\right\| f_{\beta_{Ni}}\left(\theta_i-\hat{\theta}_i\right),\\ \dot{\tilde{\xi}}_i &= \frac{\partial\xi_i}{\partial s_i}\left(f_{\alpha_i} f_{\beta_{Ti}} + \frac{\partial s_i}{\partial\lambda_i} f_{\alpha_i}\left\|\nabla\lambda_i\right\| f_{\beta_{Ni}}\right)\left(\theta_i-\hat{\theta}_i\right)\\ &\quad - k_2\tilde{\xi}_i - k_3\sum_{j=1}^{n} a_{ij}\left(\tilde{\xi}_i-\tilde{\xi}_j\right),\\ \dot{\hat{\theta}}_i &= \gamma\left(\nabla\Psi_i f_{\alpha_i}\left\|\nabla\lambda_i\right\| f_{\beta_{Ni}}^T + \tilde{\xi}_i\frac{\partial\xi_i}{\partial s_i} f_{\alpha_i}\right.\\ &\quad \left.\times\left(f_{\beta_{Ti}}^T + \frac{\partial s_i}{\partial\lambda_i}\left\|\nabla\lambda_i\right\| f_{\beta_{Ni}}^T\right)\right). \end{aligned} \tag{27}$$

By Assumption 3, on the set $\Omega_i$ the inequalities

$$\begin{aligned}&\left\|\nabla\lambda_i\right\| \le c_2, \quad \left|\frac{\partial\xi_i}{\partial s_i}\right| \le c_3,\\ &\left|\frac{\partial s_i}{\partial\lambda_i}\right| \le \int_0^{2\pi}\sqrt{\left(\dot{p}_{x_i}(\tau)\right)^2+\left(\dot{p}_{y_i}(\tau)\right)^2}d\tau \le c_4,\end{aligned} \tag{28}$$

hold for some positive constants $c_2$, $c_3$ and $c_4$. According to Assumption 2 and the fact that $\|N_i\| = \|T_i\| = 1$ one obtains

$$\left\|f_{\beta_{Ni}}\right\| \le c_1, \quad \left\|f_{\beta_{Ti}}\right\| \le c_1. \tag{29}$$

Let now

$$\delta_i = \theta_i - l_i. \tag{30}$$

From (28), (29) and (30) one has

$$\begin{aligned}\dot{V}_I \le &-\sum_{i=1}^{n} k_1\nabla\Psi_i f_{\alpha_i} + \sum_{i=1}^{n} c_1c_2\nabla\psi_i f_{\alpha_i}\left|\delta_i\right|\\ &-\sum_{i=1}^{n} k_2\tilde{\xi}_i^2 - \sum_{i=1}^{n} k_3\tilde{\xi}_i\sum_{j=1}^{n} a_{ij}\left(\tilde{\xi}_i-\tilde{\xi}_j\right)\\ &+\sum_{i=1}^{n} c_1c_3\left(1+c_2c_4\right)\left|\tilde{\xi}_i f_{\alpha_i}\left(\lambda_i\right)\delta_i\right|. \end{aligned} \tag{31}$$

Exploiting the inequality

$$\left|\tilde{\xi}_i f_{\alpha_i}\left(\lambda_i\right)\delta_i\right| \le \frac{1}{2}\tilde{\xi}_i^2\left|\delta_i\right|^2 + \frac{1}{2}f_{\alpha_i}^2 \tag{32}$$

By Assumption 3 $|\delta_i| \le \delta_{i*}$ we conclude that

$$\begin{aligned}\dot{V}_I \le &-\sum_{i=1}^{n} k_1\nabla\Psi_i f_{\alpha_i} + \sum_{i=1}^{n} c_1c_2\nabla\psi_i f_{\alpha_i}\delta_{i*}\\ &-\sum_{i=1}^{n} k_2\tilde{\xi}_i^2 - \sum_{i=1}^{n} k_3\tilde{\xi}_i\sum_{j=1}^{n} a_{ij}\left(\tilde{\xi}_i-\tilde{\xi}_j\right)\\ &+\sum_{i=1}^{n} c_1c_3\left(1+c_2c_4\right)\left(\frac{1}{2}\tilde{\xi}_i^2\delta_{i*}^2 + \frac{1}{2}f_{\alpha_i}^2\right) \le W_I, \end{aligned} \tag{33}$$

where

$$\begin{aligned}W_I = &-\sum_{i=1}^{n}\left(k_1 - \frac{1}{2}c_1c_3\left(1+c_3c_5\right) - c_1c_2\delta_{i*}\right)\nabla\Psi_i f_{\alpha_i}\\ &-\sum_{i=1}^{n}\frac{1}{2}c_1c_3\left(1+c_2c_4\right)\left(\nabla\Psi_i f_{\alpha_i} - f_{\alpha_i}^2\right)\\ &-\sum_{i=1}^{n}\left(k_2 - \frac{1}{2}c_1c_3\left(1+c_2c_4\right)\delta_{i*}^2\right)\tilde{\xi}_i^2\\ &-\frac{1}{2}\sum_{i=1}^{n} k_3\sum_{j=1}^{n} a_{ij}\left(\tilde{\xi}_i-\tilde{\xi}_j\right)^2. \end{aligned}$$

Selecting

$$\begin{aligned}k_1 &> \frac{1}{2}c_1c_3\left(1+c_2c_4\right) + c_1c_2\delta_{i*},\\ k_2 &> \frac{1}{2}c_1c_3\left(1+c_2c_4\right)\delta_{i*}^2, \end{aligned} \tag{34}$$

recalling Assumption 1 and inequality (33), we conclude that $\dot{V}_I \le 0$, which yields the following result.

*Theorem 1:* Consider the family of level orbits characterized in Lemma 1. Suppose that the initial positions of each vehicle is such that $p_i(0) \in \Omega_i$. Assume moreover that Assumptions 1 to 4 hold. Then Problem 1 is solved by the formation tracking control law

$$u_i = \begin{bmatrix} N_i^T \\ T_i^T \end{bmatrix}^{-1}\begin{bmatrix} v_{N_i} \\ v_{T_i} \end{bmatrix} \tag{35}$$

with $v_{N_i}$, $v_{T_i}$ and the adaptive update law $\dot{\hat{\theta}}_i$ given in (23), (24) and (25), respectively.

*Proof:* Let $p_i(0) \in \Omega_i$ and note that the set $\Phi_I = \left\{\left(\lambda_i, \tilde{\xi}_i, l_i - \hat{\theta}_i\right) | V_I \leqslant c_5\right\}$, for some $c_5 > 0$, is closed by continuity. Note now that $|\lambda_i| < \varepsilon_i$, $\left|\tilde{\xi}_i\right| \leqslant \sqrt{2c_5}$ and $\left|l_i - \hat{\theta}_i\right| \leqslant \sqrt{2\gamma c_5}$. Thus the set $\Phi_I$ is compact. As a result the closed-loop system (27) is Lipschitz continuous on the set $\Phi_I$ and also piecewise continuous in $t$, which implies that for each initial condition there exists a unique solution..

Note that the value of $V_I$ is non-increasing along the trajectories of the system. When the initial value of $V_I$ is finite, the entire solution stays in $\Phi_I$, which implies that $|\lambda_i(p_i(t))| < \varepsilon_i$ by conditions (C4) and (C5). By LaSalle-Yoshizawa Theorem we have that

$$\lim_{t\to+\infty} W_I(t) = 0,$$

that is

$$\lim_{t\to+\infty}\nabla\Psi_i(t) f_{\alpha_i}\left(\lambda_i(t)\right) = 0, \tag{36}$$

$$\lim_{t\to\infty}\tilde{\xi}_i(t) = \lim_{t\to\infty}\left(\xi_i(t) - \xi_*(t)\right) = 0, \tag{37}$$

where $\xi = [\xi_1, \cdots, \xi_n]^T$. From (36), (C6) and Assumption 1, we therefore conclude that $\lim_{t\to+\infty}\lambda_i(t) = 0$. ■

### C. Solution to Problem 2

To deal with Problem 2 the term $\frac{1}{2}\sum_{i=1}^{n}\tilde{\xi}_i^2$ in the candidate Lyapunov function is replaced by $\frac{1}{4}\sum_{i=1}^{n}\sum_{j=1}^{n} a_{ij}\left(\xi_i-\xi_j\right)^2$, that is

$$\begin{aligned}V_{II} = &\sum_{i=1}^{n}\Psi\left(\lambda_i\right) + \frac{1}{4}\sum_{i=1}^{n}\sum_{j=1}^{n} a_{ij}\left(\xi_i-\xi_j\right)^2\\ &+\frac{1}{2\gamma}\sum_{i=1}^{n}\left(l_i-\hat{\theta}_i\right)^T\left(l_i-\hat{\theta}_i\right). \end{aligned} \tag{38}$$

Taking the time derivative of (38) along the trajectories of the system yields

$$\begin{aligned}\dot{V}_{II} = &\sum_{i=1}^{n}\nabla\Psi_i\left[\left\|\nabla\lambda_i\right\| v_{N_i} + f_{\alpha_i}\left\|\nabla\lambda_i\right\| f_{\beta_{Ni}}\left(\theta_i - l_i \ \ +\hat{\theta}_i\right)\right]\\ &+\sum_{i=1}^{n}\frac{\partial\xi_i}{\partial s_i}\left(v_{T_i} + \frac{\partial s_i}{\partial\lambda_i}\left\|\nabla\lambda_i\right\| v_{N_i} + f_{\alpha_i}\left(f_{\beta_{Ti}}\right.\right.\\ &\left.\left.+\frac{\partial s_i}{\partial\lambda_i}\left\|\nabla\lambda_i\right\| f_{\beta_{Ni}}\right)\left(\theta_i - l_i + \hat{\theta}_i\right)\right)\sum_{j=1}^{n} a_{ij}\left(\xi_i-\xi_j\right) \end{aligned}$$

$$+\sum_{i=1}^{n}\left(l_i-\hat{\theta}_i\right)^T\left[-\frac{1}{\gamma}\dot{\hat{\theta}}_i+\nabla\Psi_i f_{\alpha_i}(\lambda_i)\|\nabla\lambda_i\| f_{\beta Ni}^T\right.$$
$$\left.+\frac{\partial\xi_i}{\partial s_i}f_{\alpha_i}\left(f_{\beta Ti}^T+\frac{\partial s_i}{\partial\lambda_i}\|\nabla\lambda_i\| f_{\beta Ni}^T\right)\sum_{j=1}^{n}a_{ij}(\xi_i-\xi_j)\right]. \quad (39)$$

To guarantee that $\dot{V}_{II}\leq 0$ one selects $v_{N_i}$ as in (23) and

$$v_{T_i}=-f_{\alpha_i}\left(f_{\beta Ti}+\frac{\partial s_i}{\partial\lambda_i}f_{\alpha_i}\|\nabla\lambda_i\| f_{\beta Ni}\right)\hat{\theta}_i$$
$$-\frac{\partial s_i}{\partial\lambda_i}\|\nabla\lambda_i\| v_{N_i}-\left(\frac{\partial\xi_i}{\partial s_i}\right)^{-1}k_2\sum_{j=1}^{n}a_{ij}(\xi_i-\xi_j), \quad (40)$$

$$\dot{\hat{\theta}}_i=\gamma f_{\alpha_i}\|\nabla\lambda_i\| f_{\beta Ni}^T+\gamma\frac{\partial\xi_i}{\partial s_i}f_{\alpha_i}\left(f_{\beta Ti}^T+\frac{\partial s_i}{\partial\lambda_i}\|\nabla\lambda_i\| f_{\beta Ni}^T\right)$$
$$\times\sum_{j=1}^{n}a_{ij}(\xi_i-\xi_j). \quad (41)$$

Exploiting the inequality

$$\left|f_{\alpha_i}\delta_i\sum_{j=1}^{n}a_{ij}(\xi_i-\xi_j)\right|\leq\frac{1}{2}|\delta_i|^2\left(\sum_{j=1}^{n}a_{ij}(\xi_i-\xi_j)\right)^2+\frac{1}{2}f_{\alpha_i}^2 \quad (42)$$

and substituting (23), (40) and (41) into (39) yields

$$\dot{V}_{II}\leq-\sum_{i=1}^{n}\left(k_1-\frac{1}{2}c_1c_3(1+c_2c_4)-c_1c_2\delta_{i*}\right)\nabla\Psi_i f_{\alpha_i}$$
$$-\sum_{i=1}^{n}\frac{1}{2}c_1c_3(1+c_2c_4)\left(\nabla\Psi_i f_{\alpha_i}-f_{\alpha_i}^2\right)$$
$$-\sum_{i=1}^{n}\left(k_2-\frac{1}{2}c_1c_3(1+c_2c_4)\delta_{i*}^2\right)\left(\sum_{j=1}^{n}a_{ij}(\xi_i-\xi_j)\right)^2. \quad (43)$$

Choosing $k_1$ and $k_2$ to satisfy inequality (34) yields $V_{II}\leq 0$, hence the following result.

*Theorem 2:* Consider the family of level orbits characterized in Lemma 1. Suppose that the initial positions of each vehicle is such that $p_i(0)\in\Omega_i$. Assume moreover that Assumptions 1 to 4 hold. Then Problem 2 is solved by the formation tracking control law (35) with $v_{N_i}$, $v_{T_i}$ and the adaptive update law $\dot{\hat{\theta}}_i$ given in (23), (40) and (41), respectively.

*Proof:* The proof follows the same argument as the proof of Theorem 1, hence it is omitted. ■

*Remark 6:* In Problem 1 the formation control law $v_{T_i}$ in (24) is designed on the basis of the reference orbital speed $\eta_*$, its integral $\xi_*$ and the consensus errors $\sum_{j=1}^{n}a_{ij}(\xi_i-\xi_j)$. On the other hand the design of the parameter update law $\dot{\hat{\theta}}_i$ in (25) does not use any neighboring states. In Problem 2 the design of $v_{T_i}$ in (40) is independent of the reference orbital speed and the parameter update law $\dot{\hat{\theta}}_i$ in (41) is designed according to the consensus errors $\sum_{j=1}^{n}a_{ij}(\xi_i-\xi_j)$.

## IV. Simulation

Two examples to illustrate the results in Theorem 1 and 2, respectively are presented. The topology among the vehicles is as shown in Figure 4. The vehicles are required to form an in-line formation pattern under the effect of the spatio-temporal rotating flowfield described by equation (8) with $f_{\alpha_i}=0.1\lambda_i$, $f_{\beta_i}=diag(\cos 0.1t,\sin 0.1t)$ and the unknown time-varying parameters $\theta_i(t)=[\theta_{x_i},\theta_{y_i}]^T=[\sin 0.1t,\cos 0.2t]^T$.

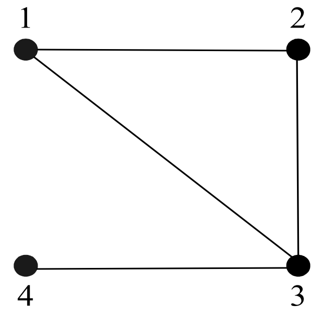


Fig. 4. Bidirectional graph.

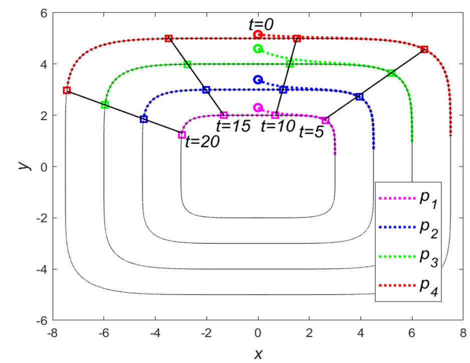


Fig. 5. Motion of the vehicles.

**Case 1:** The orbits are concentric superellipses with different semi-major axis and semi-minor axis, that is

$$C_{i0}:\left(\frac{p_{x_i}}{e_i a}\right)^6+\left(\frac{p_{y_i}}{e_i b}\right)^6=1,$$

where $e_i=1+0.5(i-1)$, $a=3$, $b=2$, $i=1,2,3,4$. The control gains are selected as $k_1=200$, $k_2=4$, $k_3=5$. We use the formation tracking algorithm given in Theorem 1 to achieve in-line formation motion around the given orbit with reference orbital speed $\eta_*=0.4$. The motion of the vehicles is illustrated in Figure 5. From this figure one can see that the four vehicles converge to the given orbits and form the desired formation. The time histories of the path following errors $\lambda_i$ and of the formation errors $\xi_i-\xi_j$ are plotted in Figures 6 and 7, respectively. The time histories of the parameter estimates $\hat{\theta}_{x_i}$ and $\hat{\theta}_{y_i}$ are plotted in Figures 8 and 9, respectively. Consistently with Theorem 1, path following and formation tracking are achieved.

**Case 2:** The orbits are concentric ellipses with different semi-major axis and semi-minor axis as in Case 1. The control gains are set to $k_1=20$, $k_2=5$. We use the formation tracking algorithm given in Theorem 2 to achieve in-line formation around the orbits without reference velocity. The motion of the vehicles, the path following errors $\lambda_i$, the formation errors $\xi_i-\xi_j$ and the parameter estimates $\hat{\theta}_{x_i}$ and $\hat{\theta}_{y_i}$ are displayed in Figures 10 to 14, respectively.

## V. Conclusion

A novel adaptive method to solve formation tracking in the presence of the unknown time-varying parameters of the spatiotemporal flowfield is proposed. According to the *congelation of variables* method the parameter update law does not rely on any restrictions on the derivatives of the unknown parameters. By integrating adaptive estimate, concentric compression and barrier functions, a formation tracking control law to achieve both path following and a formation

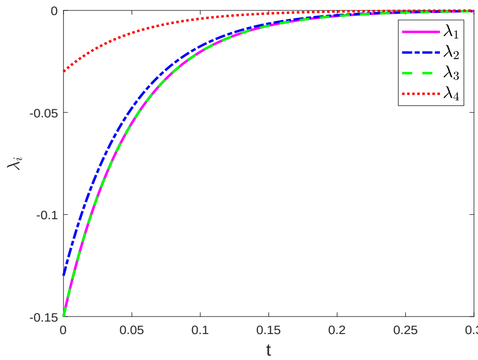


Fig. 6. Time histories of the path following errors.

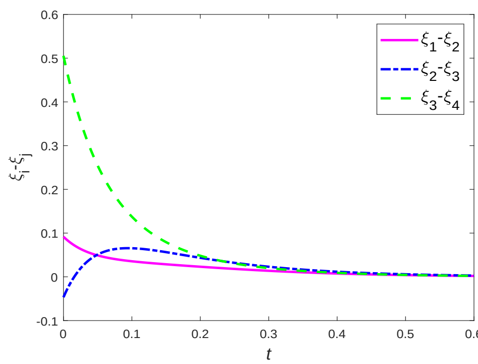


Fig. 7. Time histories of the formation errors.

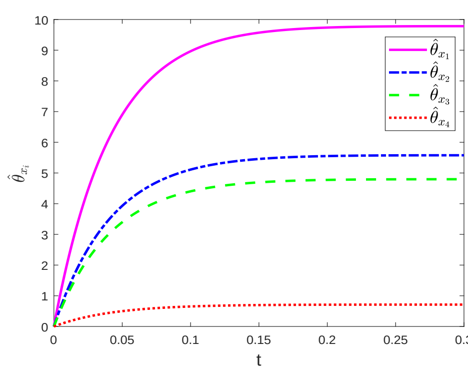


Fig. 8. Time histories of the parameter estimates $\hat{\boldsymbol{\theta}}_{\boldsymbol{x_i}}$.

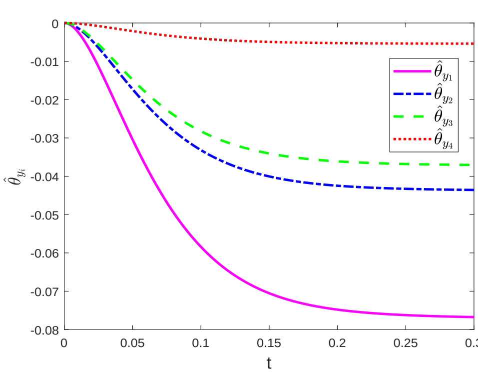


Fig. 9. Time histories of the parameter estimates $\hat{\boldsymbol{\theta}}_{\boldsymbol{y_i}}$.

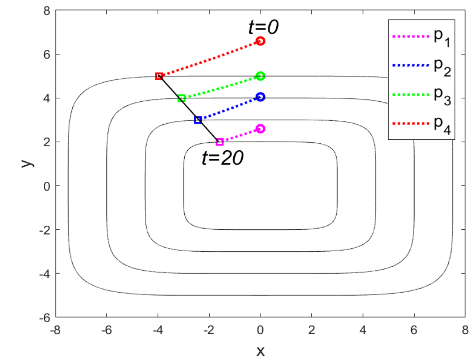


Fig. 10. Movement of the vehicles.

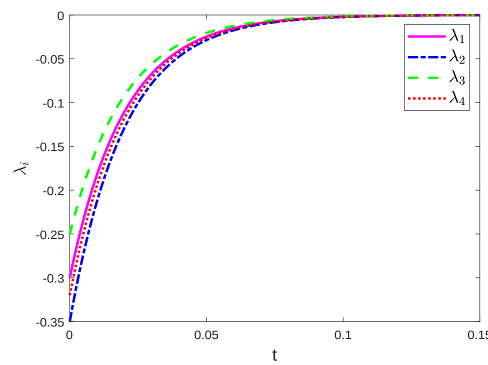


Fig. 11. Time histories of the path following errors.

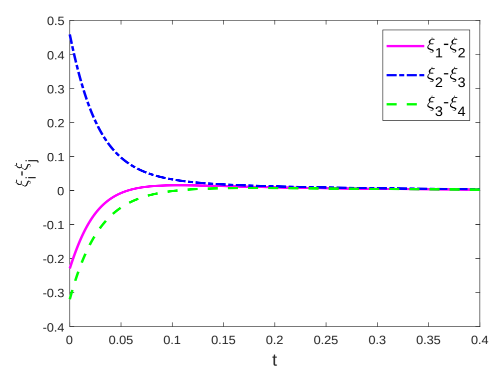


Fig. 12. Time histories of the formation errors.

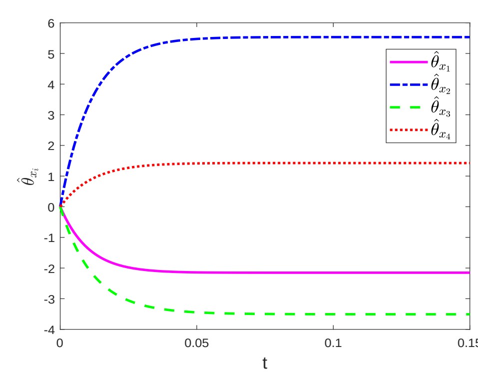


Fig. 13. Time histories of the parameter estimates $\hat{\boldsymbol{\theta}}_{\boldsymbol{x_i}}$.

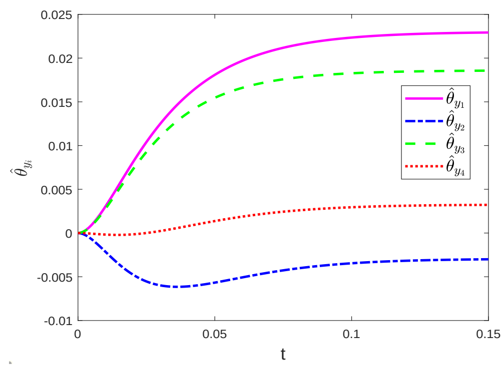


Fig. 14. Time histories of the parameter estimates $\hat{\boldsymbol{\theta}}_{\boldsymbol{y_i}}$.

moving along the desired orbits with bounded reference orbital speed is designed at first. Then formation tracking motion without reference orbital speed is achieved by using the state of the neighboring vehicles. Conditions on the control gains to guarantee that the path following errors and formation errors asymptotically converge to zeros are presented.

In future work formation tracking problems with directed or time-varying topologies will be considered.

## References


[1] R. W. Beard, J. Lawton, and F. Y. Hadaegh, "A coordination architecture for spacecraft formation control," *IEEE Trans. Control Syst. Technol.*, vol. 9, no. 6, pp. 777–790, 2001.

[2] E. Fiorelli, N.E. Leonard, P. Vhatta D.A. Paley, R. Bachmayer, D.M. Fratantoni, "Multi-AUV control and adaptive sampling in Monterey Bay," *IEEE J. Ocean. Eng.*, vol. 31, no. 4, pp. 935–948, 2006.

[3] Y. Cao, W. Ren, "Distributed coordinated tracking with reduced interaction via a variable structure approach," *IEEE Trans. Autom. Control*, vol. 57, no. 1, pp. 33–48, 2001.

[4] Z. Lin, B. Francis, M. Maggiore, "Necessary and sufficient graphical conditions for formation control of unicycles," *IEEE Trans. Autom. Control*, vol. 50, no. 1, pp. 121–125, 2005.

[5] A.L. Bertozzi, M. Kemp, D. Marthaler, "Determing enviromental boundaries: asynchronous communication and physical scales," in *Cooperative Control. Lecture Notes in Control and Information Sciences*, 1st ed., vol. 309, V. Kumar, N. Leonard, A.S. Morse, Ed. Germany: Springer, 2005, pp. 25–42.

[6] R. Ghabcheloo, "Coordinated path following of multiple autonomous vehicles," Ph.D. dissertation, Dept. Syst. Robot. Lisbon Univ., Portugal, 2007.

[7] F. Zhang and N. E. Leonard, "Coordinated patterns of unit speed particles on a closed curve," *Syst. Control Lett.*, vol. 56, no. 6, pp. 397–407, 2007.

[8] Y.-Y. Chen, Y.-P. Tian, "Formation tracking and attitude synchronization control of underactuated ships along closed orbits," *Int. J. Robust Nonlin.*, vol. 25, no. 16, pp. 3023–3044, 2015.

[9] R. Zheng, Z. Lin, M. Fu, D. Sun, "Distributed control for uniform circumnavigation of ring-coupled unicycles," *Automatica*, vol. 53, pp. 23–29, 2015.

[10] N.E. Leonard, D.A. Paley, F. Lekien, R. Sepulchre, D.M. Fratantoni, R.E. Davis, "Collective motion, sensor networks, and ocean sampling," *Proc. IEEE Inst. Electr. Electron. Eng.*, vol. 95, no. 1, pp. 48–74, 2007.

[11] N. Sydney, G. Smyth, D.A. Paley, "Dynamic control of autonomous quadrotor flight in an estimated wind field," in *Proc. IEEE Conf. Decision and Control*, Florence, Italy, 2013, pp. 3609–3616.

[12] D.A. Paley, C. Peterson "Stabilization of collective motion in a time-invariant flowfield," *J. Guid. Control Dyn.*, vol. 32, no. 3, pp. 771–779, 2009.

[13] C.K. Peterson and D.A. Paley, "Multivehicle coordination in an estimated time-varying flowfield," *J. Guid. Control Dyn.*, vol. 34, no. 1, pp. 177–191, 2011.

[14] C.K. Peterson and D.A. Paley, "Distributed estimation for motion coordination in an unknown spatially varying flowfield," *J. Guid. Control Dyn.*, vol. 36, no. 3, pp. 894–898, 2013.

[15] Y.-Y. Chen, X. Ai, Y. Zhang, "Spherical formation tracking control for second-order agents with unknown general flowfields and strongly connected topologies," *Int. J. Robust Nonlin.*, vol. 29, no. 11, pp. 3715–3735, 2019.

[16] X. Wang, S. Li, J. Lam, "Distributed active anti-disturbance output consensus algorithms for higher-order multi-agent systems with mismatched disturbances," *Automatica*, vol. 71, pp. 30–37, 2016.

[17] S. Ghapani, S. Rahili, W. Ren, "Distributed average tracking of physical second-order agents with heterogeneous unknown nonlinear dynamics with contraint on input signals," *IEEE Trans. Autom. Control*, vol. 64, no. 3, pp. 1178–1184, 2019.

[18] Y. Dong, Jie Chen, J. Huang, "Cooperative robust output regulation for second-order nonlinear multiagent systems with an unknown exosystem," *IEEE Trans. Autom. Control*, vol. 63, no. 10, pp. 3418–3425, 2018.

[19] J. Guo, G. Yan, Z. Lin, "Local control strategy for moving-target-enclosing under dynamically changing network topology," *Syst. Control Lett.*, vol. 59, no. 10, pp. 654–661, 2010.

[20] B.S. Kim, A.J. Calise, "Nonlinear flight control using neural networks," *J. Guid. Control Dyn.*, vol. 20, no. 1, pp. 26–33, 1997.

[21] P. Gurfil, M. Idan, N.J. Kasdin, "Adaptive neural control of deep-space formation flying," *J. Guid. Control Dyn.*, vol. 26, no. 3, pp. 491–501, 2003.

[22] Z. Peng, D. Wang, Z. Chen, X. Hu, W. Lan, "Adaptive dynamic surface control for formations of autonomous surface vehicles with uncertain dynamics," *IEEE Trans. Control Syst. Technol.*, vol. 21, no. 2, pp. 513–520, 2013.

[23] Z. Peng, D. Wang, H. Wang, W. Wang, "Coordinated formation pattern control of multiple marine surface vehicles with model uncertain and time-varying ocean currents," *Neural Comput. Applic.*, vol. 25, no. 7-6, pp. 1771–1783, 2014.

[24] C.L.P. Chen, G.-X. Wen, Y.-J Liu, F.-Y. Wang "Adaptive consensus control for a class of nonlinear multiagent time-delay systems using neural networks," *IEEE Trans. Neural Netw. Learn. Syst.*, vol. 25, no. 6, pp. 1217-1226, 2014.

[25] J.L. Yu, X.W. Dong, Q.D. Li, Z. Ren, "Practical time-varying formation tracking for second-order nonlinear multiagent systems with multiple leaders using adaptive neural networks," *IEEE Trans. Neural Netw. Learn. Syst.*, vol. 29, no. 12, pp. 6015–6025, 2018.

[26] Z. Jia, L. Wang, J. Yu, X. Ai, "Distributed adaptive neural networks leader-following formation control for quadrotors with directed switching topologies," *ISA Trans.*, vol. 93, pp. 93–107, 2019.

[27] K.M. Lynch, I.B. Schwartz, P. Yang, R.A. Freeman, "Decentralized environmental modeling by mobile sensor networks," *IEEE Trans. Robot.*, vol. 24, no. 3, pp. 710–724, 2008.

[28] K. Chen, A. Astolfi, "Adaptive control of linear systems with time-varying parameters," in *Proc. 2018 Amer. Control Conf.* IEEE, pp. 80–85.

[29] K. Chen, A. Astolfi, "I&I adaptive control for systems with varying parameters," *in Proc. IEEE Conf. Decision and Control*. IEEE, 2018, pp. 2205–2210.

[30] K. Chen, A. Astolfi, "Output-feedback adaptive control for systems with time-varying parameters," *IFAC-PapersOnLine*, vol. 52, no. 16, pp. 586–591, 2019.

[31] K. Chen, A. Astolfi, "Adaptive control for systems with time-varying parameters," *IEEE Trans. Autom. Control*, available online: DOI:10.1109/TAC.2020.3046141, 2021.

[32] Y.-Y. Chen, Y. Zhang, Z.-Z. Wang, "An adaptive backstepping design for formation tracking motion in an unknown eulerian specification flowfield," *J. Franklin I.*, vol. 354, no. 14, pp. 6217–6233, 2017.